Macro- and microscale structure formation and aging in different arrested states of Laponite dispersions

M. Pilavtepe,[1,a)] S. M. Recktenwald,[1] R. Schuhmann,[2] K. Emmerich,[2] and N. Willenbacher[1]

[1]*Institute for Mechanical Process Engineering and Mechanics, Karlsruhe Institute of Technology, 76131 Karlsruhe, Germany*

[2]*Competence Center for Material Moisture, Karlsruhe Institute of Technology, 76344 Karlsruhe, Germany*

(Received 24 August 2017; final revision received 28 January 2018; published 26 February 2018)

Abstract

Structure formation and aging in different arrested states of Laponite dispersions have been investigated at the macro- and microscale. Covering a wide range of solid content and salt concentrations at different *p*H glasses, strong and weak gels with prevailing edge-to-face (EF) or face-to-face (FF) layer contacts were formed. Mechanical shear and squeeze flow rheometry were combined with diffusing wave spectroscopy and multiple particle tracking (MPT) microrheology. Strong attractive gels form much more quickly than weak gels, and particularly repulsive glasses. Gels with preferred EF contacts are stronger and are created more quickly than gels with prevailing FF contacts. Strong gels show little aging and exhibit a weak increase of $G' \sim t^{\alpha}$ with $\alpha = 0.11 \pm 0.03$, higher α values are found for weak gels, and the strongest aging is observed in glasses. MPT data reveal structural refinement at the submicrometer length scale during aging for gels but not for glasses. Strong structural heterogeneity most pronounced at $p\mathrm{H} = 8.5$ occurs during gel or glass formation, but at longer times, all arrested states appear homogenous at the 0.2 μm length scale. Finally, all arrested states exhibit power law frequency dependence $G'' \sim \omega^{0.75}$ at high frequencies attributed to internal bending modes of layers. © *2018 The Society of Rheology*.
https://doi.org/10.1122/1.5001382

I. INTRODUCTION

The phase behavior, structure and dynamics of clay mineral colloidal dispersions are of high technical relevance and great scientific interest. Engineering challenges include soil mechanics, application of construction materials or processing of pastes including clay mineral particles as additives. The variety of different dynamically arrested states observed in such systems has stimulated the interest of soft matter scientists. Fundamental investigations address phase behavior and particularly structure and dynamics of different arrested states [1–7]. These features are controlled by the strength and range of electrostatic interactions among particles strongly varying with *p*H and added electrolyte as schematically sketched in Fig. 1. Laponite dispersions have been investigated as a model system for clay mineral suspensions [8] and disklike colloids [9–11] in general. Laponite is a synthetic hectorite, and the platelike particles carry permanent negative charges due to isomorphic substitution. Edges are positively charged at low *p*H, but negative edge charges occur at high *p*H. The point of zero charge at edges, $p\mathrm{H}_{\mathrm{PZC,edge}}$, is reported to be approximately $p\mathrm{H} = 11$ [12]. Even if the inherent *p*H of Laponite dispersion is lower than its $p\mathrm{H}_{\mathrm{PZC,edge}}$, in the absence of ions or at very low ionic strength, the extended electrical double layer around the dispersed layers leads to the formation of an arrested glass structure [1,3,13,14]. Setting *p*H or adding an electrolyte leads to a contraction of the electrical double layer, allowing for direct layer contacts, and so-called attractive arrested states, also termed gels, are formed [1,3]. At $p\mathrm{H} > p\mathrm{H}_{\mathrm{PZC,edge}}$, face-to-face [12] (FF) and/or edge-to-edge [15] (EE) contacts with Na^+ in between are formed, resulting in a so-called partially parallel overlapped (PPO) gel structure [16,17]. At high *p*H and high electrolyte concentration, the possibility of FF layer orientation is higher than EE interaction [15]. At $p\mathrm{H} < p\mathrm{H}_{\mathrm{PZC,edge}}$, edges and faces are oppositely charged, and edge-to-face (EF) contacts occur, which are supposed to result in arrested gel states with a so-called house of cards (HOC) structure [18–21]. Models for structure formation in clay mineral dispersions are often based on these assumptions about different types of particle contacts mentioned above. The existence of so-called PPO or HOC structures is widely accepted in the clay mineral science community [12,14,15,18,22–25]. However, there is no direct experimental evidence for these particle contacts except for Monte Carlo simulations [19] regarding gelation in clay mineral suspensions considering electrostatic interactions among the platelike particles and cryo-TEM 3D-images of smectite particles in aqueous environment [24]. The physical motivation for these structural models is the experimental fact that the rim or edge charge changes from positive at $p\mathrm{H} < p\mathrm{H}_{\mathrm{PZC,edge}}$ to negative at higher *p*H. The edge charge of Laponite has been quantitatively determined using potentiometric and mass titration techniques [26].

[a)]Author to whom correspondence should be addressed; electronic mail: muege.pilavtepe@kit.edu

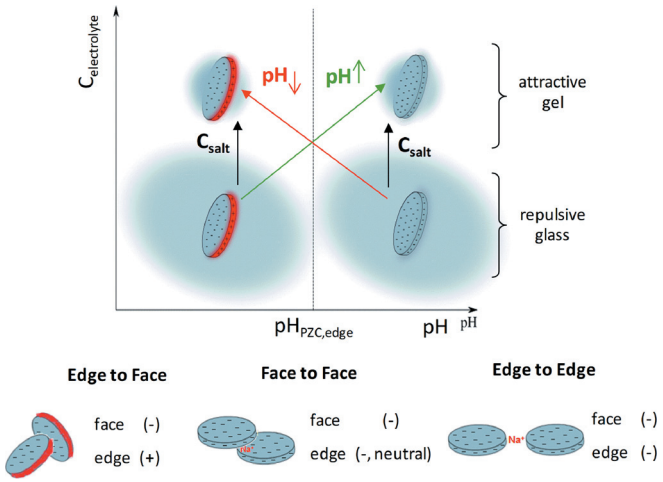

FIG. 1. Effect of electrolyte concentration and *p*H on surface charge and range of electrical double layer in aqueous Laponite dispersions. Negative charges are marked in blue, positive charges in red. The different pathways of changing surface charge and electrostatic interaction are marked by arrows.

Structure formation and aging in clay mineral dispersions strongly depend on particle and salt concentration [7,27]. Due to the short-range attractive forces among Laponite layers, gel structures form more quickly than glass structures built by long-range repulsive forces [3].

The kinetics of the gel/glass formation in Laponite dispersions at different solids content and electrolyte concentration has been studied by numerous authors covering time intervals from hours to years using light and X-ray scattering [5,27–31] as well as rheological methods [13,32–37]. Willenbacher [36] found a power law relationship between complex viscosity and time ($|\eta^*| \sim t^{0.13\pm0.02}$) for gel-like Laponite dispersions holding within the time regime up to 10^6 s. As noted by Ruzicka and Zaccarelli [6], a deficiency of some other early studies on Laponite phase behavior is the neglect of sample aging [4,38], which may have led to inaccurate interpretation of arrested states of dispersions. Therefore, many different phase diagrams of Laponite dispersions are available [3,4,7,29,39]. Hence, a clear picture of layer interaction at different *p*H, electrolyte concentration, and the influence of electrolyte concentration on the kinetics of phase transition of Laponite dispersion is still lacking.

Laponite dispersions with low solid concentration and without added salt need more time to reach an arrested state, and cluster size changes during this time. Therefore, such dispersions are called heterogeneous gels at a macroscopic length scale [28]. At higher clay mineral concentration, the arrested state forms more quickly, and there is no evidence for structural heterogeneity from dynamic light or small X-ray scattering; accordingly, such states are called homogeneous gel or attractive glass [28,30]. On the other side, microrheological studies using particle tracking methods revealed that heterogeneous gel-like structures occur in Laponite dispersions at low solids and high electrolyte concentration [32,40], and homogeneous repulsive glass structures were observed in the absence of electrolyte [33]. Oppong *et al.* [32] observed an increase of heterogeneity during structure formation until the characteristic crossover time at which $G' = G''$ was reached with no further change beyond that time. Their results, however, may be obscured by aging effects as they added the tracer particles one month after sample preparation, assuming that complete rejuvenation is possible by vigorous sonication. Rich *et al.* [40] observed a gradual shift of sol-gel transition in their particle tracking experiments depending on the size of the used tracer particles and found an increase in heterogeneity up to the crossover time but did not continue to monitor this at longer times. Jabbari-Farouji *et al.* [33] claimed that glass Laponite dispersions are homogeneous based on microrheological experiments using probe particles with 1.16 μm diameter but observed heterogeneity in the gel they investigated using 0.5 μm probe particles. However, this optical tweezer-based study suffers from poor statistical significance, since the viscoelastic response of the gel sample was probed only at 5–8 different positions.

Here, we have used classical oscillatory shear rheometry and multiple particle tracking optical (MPT) microrheology to characterize kinetics of structure formation and aging for different types of repulsive or attractive arrested states. We have investigated Laponite dispersions with a broad range of clay mineral content (1–3 wt. %), added salt concentration (up to 10^{-2} M NaCl) and different *p*H (8.5, 10, and 12). The variety of methods applied in this study and the broad range of physicochemical parameters investigated provide a comprehensive scientific view of differences between arrested states with different Laponite layer orientations. A distinction between repulsive glasses and attractive gels from bulk rheological measurements alone is not trivial and sometimes may be impossible [41]. Therefore, we have combined bulk rheology with microrheology to shed new light on the long-standing controversy about the rheological behavior of Laponite dispersions at the macro- and microlength scales. We discuss the effect of the main control parameters—i.e., clay mineral content and salt concentration, as well as *p*H on kinetics of structure formation, aging, mechanical strength, microscopic heterogeneity and structural refinement for different attractive and repulsive arrested states. Beyond that, we have employed squeeze flow mechanical rheometry and diffusing wave spectroscopy (DWS) optical microrheology to determine linear viscoelastic properties in the frequency range up to 10^6 rad/s. We have investigated Laponite dispersions at various *p*H and electrolyte concentrations.

II. MATERIALS AND METHOD

A. Materials

The synthetic hectorite Laponite RD (registered trademark of BYK Additives) was donated by BYK Additives & Instruments, Germany. Its general formula is $Na_{0.38}Si_8(Mg_{5.72}Li_{0.18})O_{20}(OH)_4$. Laponite RD has a specific density of 2700 kg/m^3, specific surface area of 370 m^2/g, and cation exchange capacity (CEC) of 79 cmol (+)/kg determined according to Meier and Kahr [42] and Delavernhe *et al.* [43]. Laponite consists of a delaminated state of nearly monodisperse, rigid, disk-shaped layers with a thickness slightly less than 1 nm and a diameter of approximately 30 nm [38,39].

B. Sample preparation

The effect of solids content and added salt concentration on the flow behavior of Laponite suspensions was studied in the range of 1–3 wt. % and 0–10^{-2} M NaCl. The corresponding amount of Laponite powder was dispersed under agitation in the corresponding ionic aqueous solution. Samples were homogenized in an ultrasonic bath for 20 min. Subsequently, samples were treated in an ultrasonic homogenizer (Digital Sonifier, Branson, USA) for 20 s at 10% amplitude to ensure delamination and homogeneous distribution of clay mineral layers. During preparation, the sample temperature was kept constant at 25 °C, since heating can influence the aging behavior [44]. We measured the inherent *p*H value of Laponite dispersions as 10 ± 0.2. The *p*H value was set to $p\mathrm{H} = 12$ and $p\mathrm{H} = 8.5$ by adding 1 M NaOH or HCl aqueous solution to the initial dispersion at $p\mathrm{H} = 10$. The minimal *p*H was set to 8.5 since at lower *p*H, Laponite starts to dissolve. The rate of this reaction decreases with increasing *p*H and is negligible for $p\mathrm{H} \geq 8.5$ [5]. Samples with high salt concentration, approximately 10^{-2} M, became turbid after setting the *p*H value to 8.5. Such unstable samples were excluded from this study. No turbidity was observed for samples at $p\mathrm{H} = 12$. We checked *p*H values of all samples for a period of four months, and in accordance with Mongondry *et al.* [5], we observed that *p*H remained constant. The samples were individually prepared for each set of experiments using the same procedure. The electrolyte concentration of dispersion increases upon setting *p*H and additionally by released exchangeable cations from the Laponite structure. The *p*H-dependent CEC of Laponite corresponding to the layer charge was characterized in a wide range of *p*H by Delavernhe *et al.* [45]. The thickness of the electrical double layer (nm) can be estimated via Eq. (1) from the equivalent NaCl concentration of samples [46] calculated from conductivity of dispersions (see Table I)

$$\kappa^{-1} = \frac{0.304}{\sqrt{C_{NaCl,eq.}}}. \quad (1)$$

The composition, physicochemical properties, and the type of arrested state of all investigated samples are listed in Table I. This table also gives an overview in which figure results for each sample can be found.

C. Transient oscillatory shear at fixed frequency and amplitude

A controlled stress rheometer (HAAKE Rheostress RS 150, Thermo HAAKE, Germany) equipped with a Searle system that consists of a concentric cylinder system with rotating inner cylinder radius $R_1 = 19.36$ mm and outer cylinder radius $R_2 = 20$ mm was used to measure the structure formation and aging dynamics of Laponite dispersions. Directly after sample preparation in sol-state, 10 ml dispersions were filled into the Searle system and sheared at sufficiently high shear stress σ (greater than the apparent yield stress σ_y) for a given time interval $\Delta t = 300$ s that guarantees complete destruction of the possible sample structure. Subsequent recovery of the remaining structure was monitored using small-amplitude oscillatory shear measurements at a stress amplitude of $\sigma_0 = 0.2$ Pa and a frequency of $\omega = 0.6$ rad/s. The top of the sample chamber was covered with a plate to suppress evaporation of water.

D. Amplitude sweep experiments

We applied amplitude sweep experiments at time intervals of one week for a total lag time of up to 16 weeks to characterize the long-term aging and change of mechanical strength of Laponite dispersions. These experiments were carried out using a Physica Anton Paar MCR501 controlled stress rheometer with cone-plate geometry (diameter 25 mm, cone angle

TABLE I. Properties of investigated Laponite dispersions. The supposed structure type of dispersions (EF or FF) is shown in brackets together with the dispersion state (glass, weak or strong gel). The last column shows the numbers of the figures in which data for the respective sample are included.

Solids content (wt. %)	Added NaCl conc. (M)	*p*H	State of dispersion	Conductivity (μS cm^{-1})	Calculated electrolyte conc. (M)	Shown in Figure
1	10^{-2}	10	Strong gel (EF)	1368	1.4×10^{-2}	3(b), 5, 9(b)
1	10^{-2}	12	Weak gel (FF)	2783	3.0×10^{-2}	3(b)
2	0	10	Repulsive glass	505	3.1×10^{-3}	2(a), 2(b), 3(a), 5, 6, 9(a)
2	0	8.5	Strong gel (EF)	892	7.8×10^{-3}	3(a), 6
2	0	12	Weak gel (FF)	1869	1.9×10^{-2}	3(a), 6
2	10^{-2}	10	Strong gel (EF)	1651	1.7×10^{-2}	2(a), 2(b), 5, 9(b)
2	10^{-2}	12	Strong gel (FF)	3066	3.4×10^{-2}	5
2	10^{-3}	10	Repulsive glass	743	6×10^{-3}	2(b), 6
2	10^{-3}	8.5	Strong gel (EF)	978	8.8×10^{-3}	6
2	10^{-3}	12	Weak gel (FF)	2893	3.2×10^{-2}	6
2	10^{-4}	10	Repulsive glass	550	3.6×10^{-3}	2(b), 4(a), 5, 9(b)
2	10^{-4}	8.5	Strong gel (EF)	825	7.0×10^{-3}	4(b), 5, 8(c), 9(c)
2	10^{-4}	12	Weak gel (FF)	1520	1.5×10^{-2}	4(c), 5, 8(c), 9(c)
3	0	10	Repulsive glass	735	5.9×10^{-3}	2(b), 8(a), 9(a)
3	10^{-2}	10	Strong gel (EF)	1933	2×10^{-2}	2(b)
3	10^{-3}	10	Weak gel (EF)	1110	1×10^{-2}	2(b),
3	10^{-4}	10	Weak gel (EF)	835	7.1×10^{-3}	2(b), 5, 8(b), 10

2°, gap height at the tip of cone plate geometry 47 μm). The storage (G') and loss (G'') moduli were determined by varying the shear stress amplitude from 1 to 100 Pa at a constant frequency of 6 rad/s. In preliminary tests, we performed oscillatory shear amplitude sweeps in the range of 1–100 Pa using plate-plate geometry with varying gap height, and markers at the rim were used for visual inspection of sample deformation using video imaging. No indication of the occurrence of slip during such experiments was found.

E. Frequency sweep experiments

Oscillatory shear flow experiments at varying frequencies were performed in the linear viscoelastic regime, where G' and G'' are independent of the applied stress amplitude. The experiments were carried out using a Physica Anton Paar (MCR501) controlled stress rheometer, with cone-plate geometry (diameter 25 mm, cone angle 2°, gap height at the tip of cone plate geometry 47 μm). The experiments were executed at a constant deformation amplitude of 1% from high to low frequency (60–0.006 rad/s). Preliminary amplitude sweep experiments confirmed that this deformation is within the linear viscoelastic response regime for the suspensions investigated here.

F. Oscillatory squeeze flow

The dependence of G' and G'' on angular frequency $\omega = 2\pi f$ between 10^1 and 3×10^4 rad/s was measured by squeezing samples at very low deformation (<0.1%, depending on gap height) using a customized piezo-driven axial vibrator. G' and G'' were calculated from the detected phase shift and voltage amplitude determined in experiments with and without the sample in the measuring cell as described earlier [47]. Sample deformation in these experiments was so small that the resulting data were always in the linear viscoelastic regime [47]. The gap height was adjusted to 10–100 μm depending on the sample composition using appropriate distance rings. The exact gap width was determined from preliminary calibration with a Newtonian fluid of known viscosity. The required sample volume is approximately 100 μl. To make an accurate comparison, samples aged for 10 weeks were used for these experiments and for the frequency sweep and DWS experiments.

G. DWS

DWS is an optical microrheological technique based on the thermal motion of embedded tracer particles and covers the angular frequency range from 1 to 10^6 rad/s. We used TiO_2 nanoparticles (LS Instruments AG, Fribourg, Switzerland) of 0.36 μm in diameter as tracers; 0.5 wt. % of TiO_2 particles were added during preparation of Laponite dispersions, and 800 μl samples were filled into cuvettes (Hellma, Müllheim, Germany) with 2 mm thickness. In accordance with Bonn *et al.* [34], we observed that the addition of TiO_2 particles does not affect the linear viscoelastic response of dispersions. Measurements were conducted and analyzed using a DWS ResearchLab (LS Instruments, Fribourg, Switzerland) with a multitau correlator at an acquisition time of 270 s and echo duration of 5 s. The mean square displacement (MSD) of tracer particles was calculated from the autocorrelation of the scattered light intensity, and a generalized Stokes-Einstein equation was used to determine the complex shear modulus $G^* = G' + iG''$ [48]. The MSD was calculated for lag times between 10^1 and 10^{-6} s, and data analysis was performed as described by Oelschlaeger *et al.* [49].

H. MPT

To perform MPT video microscopy, 0.01 vol. % of dragon green fluorescent polystyrene spheres of either 1.01, 0.52, 0.21, or 0.19 μm in diameter (Bang Laboratories, USA) were added to the Laponite dispersions directly after sample preparation. According to the manufacturer, tracer particles are negatively charged due to initiator sulfate groups and adsorbed ionic surfactant. Thus, these particles should not aggregate with the negatively charged clay particles, even at low *p*H when edges are positively charged the repulsion between the tracers and the negatively charged face should be dominating. To determine the significance of negatively charged tracer particles and clay mineral interactions, Rich *et al.* [40] performed solution microcalorimetry measurements using an Isothermal titration calorimeter and found that such interactions can be safely neglected. The samples including tracer particles were vortexed and homogenized for 5 min in an ultrasonic bath. They were then directly injected into a commercial rectangular capillary of 0.1 mm in thickness and 2 mm in width (CM Scientific, UK) sealed with UV-curing glue. The microscope (Axio Observer D1, Carl Zeiss) equipped with a Fluar 100×, N.A. 1.3, oil-immersion lens was focused roughly halfway into the sample, and the Brownian motion of tracer particles was monitored in a 127×127 μm field of view, at a rate of 30 frames per second (sCMOS camera Zyla X) for 1 min. The experimental setup was described in detail by Kowalczyk *et al.* [50]. For each experiment, approximately 150 particles were tracked simultaneously. After image processing (IPS Visiometrics), displacement of particle centers was monitored using a self-written MATLAB code [50] based on the widely used Crocker and Grier tracking algorithm [51]. A highly elastic tri-block-copolymer gel Pluronic F127 (BASF SE, Ludwigshafen, Germany) has been employed to determine the static error, which sets the upper limit for the storage modulus accessible with a given setup [50] and the lower limit for heterogeneity ratio to be obtained with corresponding tracer particles [52].

III. RESULTS AND DISCUSSION

A. Structure formation and initial aging in glass and gel states

To determine the kinetics of structure formation and initial aging of different arrested states of Laponite dispersions, the change of G' and G'' was measured as a function of time using small amplitude oscillatory shear measurement (stress amplitude $\boldsymbol{\sigma_0} = 0.2$ Pa, frequency $\boldsymbol{\omega} = 0.6$ rad/s). Weak and strong gel and glass structures were obtained by dissolving 3 wt. % Laponite in deionized water and aqueous NaCl solutions with varying salt concentration up to 10^{-2} M NaCl; see Fig. 2(a). Due to the high energy input during transfer of the sample into the rheometer fixture and during the initial

steady shear period, samples were in the liquid or so-called sol-state when the oscillatory shear experiments started, as confirmed by visual inspection. All samples except the one with 10^{-2} M NaCl remained in this sol-state characterized by a low G'' value until both moduli increased and finally G' exceeded G''. The characteristic point where $G' = G''$ is generally assumed to mark the formation of a percolating network [53], and the corresponding time t_c is called the crossover or gelation time. Here, we attribute it to the formation of a sample spanning the arrested state, i.e., the repulsive glass and weak gel [Fig. 2(a)]. The situation is different for the sample including 10^{-2} M NaCl. In this case, even the first modulus values accessible after approximately 50 s (corresponding to five oscillations) are orders of magnitude higher than in the sol-state with $G' > G''$ and in the subsequent time interval of approximately 10^3 min G'' remain essentially constant, whereas G' further increases without reaching a steady state [Fig. 2(a)], as expected [36]. This demonstrates again that a sample spanning the arrested state is formed, and this attractive gel-state forms orders of magnitude more quickly than the glass state. The characteristic crossover time or gelation time t_c in this latter case is clearly below 1 min and has been extrapolated here by fitting straight lines to the first three data points of the G' and G'' curves [Fig. 2(a)]. Accordingly, we estimate $t_c \approx 0.25$ min for the strong gel formation compared to $t_c \approx$ 6–8 min and $t_c \approx 400$ min for the weak gel and glass formations, respectively. Similar experiments have been performed for other clay mineral contents. As expected, arrested states generally form much more quickly at higher clay mineral content, and for both clay mineral contents, the strong gel forms much more quickly than the glass state [Fig. 2(b)]. We attribute this to the strong attractive interactions dominating at high ionic strength. The formation of so-called weak gels at intermediate electrolyte concentration occurs approximately one order of magnitude more quickly than the glass formation. We attribute this to the weaker electrostatic repulsion among 2:1 layers compared to the glass forming low ionic strength suspensions.

We distinguish between weak and strong gels with reference to t_c and ionic strength: Dispersions with intermediate t_c (corresponding to intermediate ionic strength) are called weak gels, and finally samples with high ionic strength and distinctly shorter t_c are called strong gels.

B. Effect of *p*H on structure formation and aging

We applied time-dependent oscillatory shear measurements to Laponite dispersions at $p\mathrm{H} = 8.5$, 10, and 12 to see the *p*H effect on structure formation and aging. Two different Laponite suspensions have been investigated: 2 wt. % solid content without added electrolyte and 1 wt. % solid content with 10^{-2} M NaCl. For all investigated samples, a transition to an arrested state with $G' \gg G''$ is observed. The sample with 2 wt. % Laponite without added electrolyte at its natural *p*H forms a glass, and this takes a long time ($t_c \approx 1258$ min), as discussed above. The arrested states at $p\mathrm{H} = 12$ ($t_c = 30$ min) and $p\mathrm{H} = 8.5$ ($t_c = 0.3$ min) form much more quickly (Fig. 3).

A change in *p*H of 2 wt% Laponite dispersion without added NaCl from its inherent value of $p\mathrm{H} = 10$ to $p\mathrm{H} = 8.5$ or $p\mathrm{H} = 12$ results in a strong increase in electrolyte concentration in the aqueous phase, and the electrical conductivity increases from 505 μS/cm to 892 μS/cm and 1869 μS/cm at $p\mathrm{H} = 8.5$ and $p\mathrm{H} = 12$, respectively. This leads to a substantial compression of the electrical double layer from 5.5 nm at $p\mathrm{H} = 10$ to 3.4 nm at $p\mathrm{H} = 8.5$ and 2.2 nm at $p\mathrm{H} = 12$, calculated according to Eq. (1). This compression results in the formation of attractive gel states. Moreover, it has to be considered that $p\mathrm{H}_{\mathrm{PZC,\ edge}}$ of Laponite is approximately 10–11 as deduced from stability ratio measurements [12] and confirmed by our own CEC measurements according to Meier and Kahr [42] in [45]. These results show a strong increase in CEC at $p\mathrm{H} > 10$ that indicated deprotonation of (Mg-OH-Mg) surface sites [54] and a strong increase of negative charges at the edges [45].

At $p\mathrm{H} = 8.5$, the edges are positively charged, and at $p\mathrm{H} = 12$, they are negatively charged. Accordingly, we

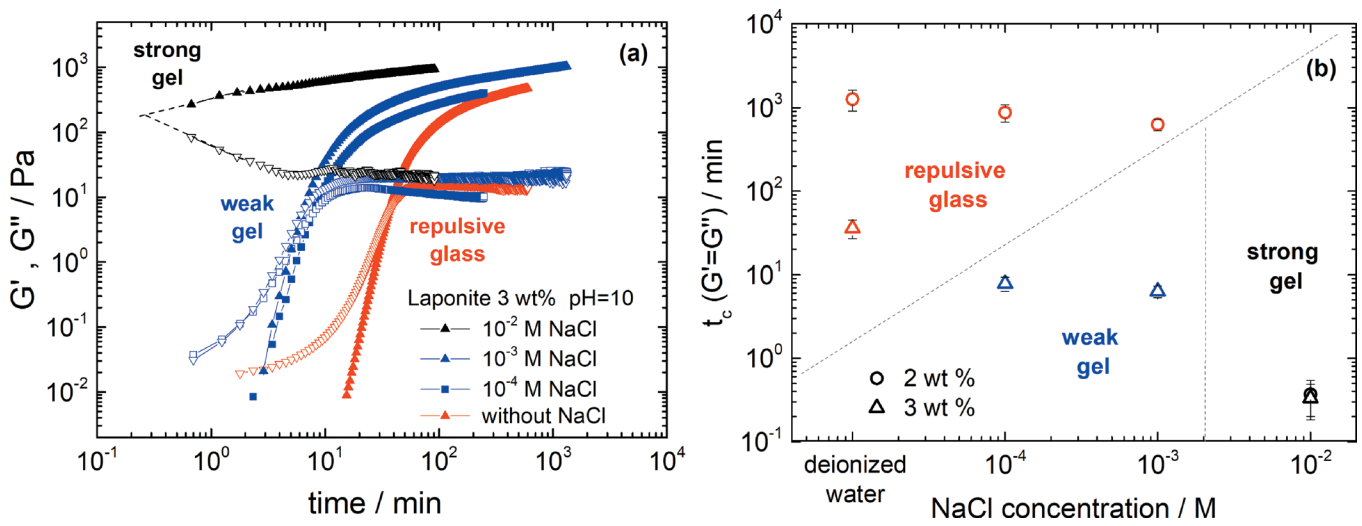

FIG. 2. (a) Structure formation for 3 wt. % Laponite dispersions at $p\mathrm{H} = 10$ with different NaCl concentration. Solid symbols = G', open symbols = G''. (b) Effect of solids content and NaCl concentration on the crossover time t_c (where $G' = G''$) of Laponite dispersions.

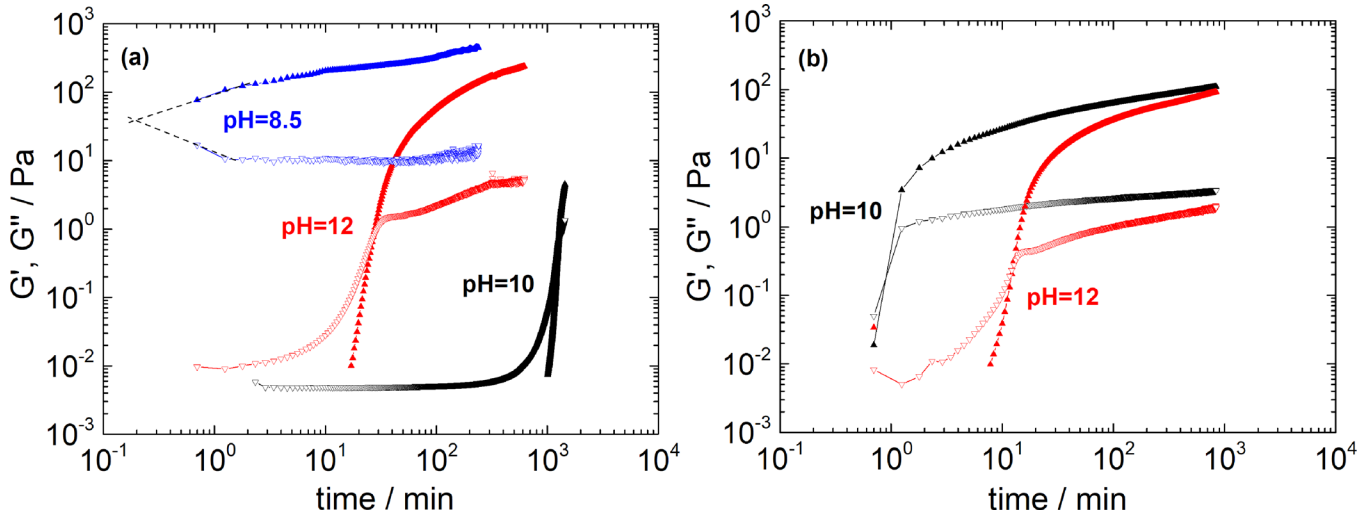

FIG. 3. Effect of *p*H on kinetics of structure formation for (a) 2 wt. % Laponite dispersion without NaCl and (b) 1 wt. % Laponite dispersion at 10^{-2} M NaCl concentration. Solid up-triangle = G', empty down-triangle = G''.

assume that EF contacts are likely to form at $p\mathrm{H} = 8.5$ and FF contacts with Na^+ in between prevail at $p\mathrm{H} = 12$. Although the electrical double layer around dispersed Laponite layers at $p\mathrm{H} = 8.5$ (≈3.4 nm) is larger than at $p\mathrm{H} = 12$ (≈2.2 nm), the structure formation is much faster at $p\mathrm{H} = 8.5$ than at $p\mathrm{H} = 12$ [Fig. 3(a)] because of the oppositely charged edges at $p\mathrm{H} = 8.5$. Therefore, we propose that structures predominantly based on EF contacts form much more quickly than FF-dominated structures. This conclusion is further corroborated by results obtained for the 2 and 1 wt. % clay mineral dispersions with 10^{-2} M NaCl. Since the kinetics of structure formation for the 2 wt. % Laponite samples are much faster than for the sample with 1 wt% solid content at high NaCl concentration, we show the effect of *p*H on structure formation here only for the 1 wt% Laponite dispersions with 10^{-2} M NaCl for the sake of clarity. Due to the high electronic concentration, attractive interactions dominate in both cases at $p\mathrm{H} = 10$ and $p\mathrm{H} = 12$, and structure formation occurs rapidly [Fig. 3(b)]. At $p\mathrm{H} = 10$, edges are still slightly positively charged, and the arrested state is assumed to have an EF structure, whereas FF contacts prevail at $p\mathrm{H} = 12$. Again, the structure supposed to be dominated by EF contacts forms more quickly than the gel including FF-type particle contacts.

C. Aging of Laponite dispersions in different arrested states

Aging—i.e., the change of structure or dynamics over long periods of time—is a common phenomenon in out-of-equilibrium systems such as amorphous polymers [55], supersaturated solid solutions [56] or clay mineral dispersions [31,36,46,57]. In the latter case, aging corresponds to a perpetual rearrangement of clay mineral layers and reorganization of the overall gel or glass structure and shows up, e.g., in a monotonic increase of the storage modulus over time. This phenomenon can already be seen from the transient G' data shown in Figs. 2 and 3 covering a time interval of approximately one day. Willenbacher [36] was the first to discuss aging in attractive gel Laponite dispersions as a self-delaying process and reported an increase of G' over several weeks following a power law $G' \sim t^{\alpha}$ with $\alpha = 0.13 \pm 0.02$ independent of clay mineral content and mechanical pretreatment of samples. Structural rearrangement and aging have been shown to endure for more than one year in dilute Laponite dispersions as revealed by light and X-ray scattering experiments [58]. Here, we have studied the aging phenomenon in different arrested states of Laponite dispersions using shear modulus measurements. We performed fixed frequency amplitude sweep oscillatory shear experiments at time intervals of one week covering a total period of up to 16 weeks. Between measurements, samples were stored in tightly sealed vials to avoid any loss of solvent. Corresponding results for dispersions including 2 wt. % Laponite and 10^{-4} M NaCl at $p\mathrm{H} = 8.5$, 10, and 12 are shown in Fig. 4. The *p*H was periodically tested and confirmed to remain at its initial value during the extended storage time.

The attractive gel formed at $p\mathrm{H} = 8.5$ and assumed to have EF particle contacts exhibits the highest strength with a shear modulus $G' \approx 10^3$ Pa. This structure also requires the largest critical stress σ_y to enable flow, usually defined as the stress amplitude at which $G' = G''$ (often also termed apparent yield stress). Here, this crossover is not visible since catastrophic failure destroys the structure, i.e., G' rapidly decays and becomes immeasurably small. The critical stress amplitude at which this occurs is thus termed σ_y and found to be ≈ 70 Pa. This structure shows very little aging, and the modulus increases by only 10% within 5 weeks of storage.

The attractive arrested state formed at $p\mathrm{H} = 12$ and supposed to have a prevailing FF structure exhibits a much weaker shear strength than the EF structure with an initial modulus $G' = 10^2$ Pa and $\sigma_y = 15$ Pa. This type of gel experiences a gradual structural breakdown when it is exceeded and aging is clearly visible, and the modulus increases by a factor of two within 5 weeks. The repulsive glass formed at $p\mathrm{H} = 10$ exhibits lower initial shear strength and yield stress than the attractive gel formed at $p\mathrm{H} = 12$. However, it exhibits uniquely strong aging, and G' increases by a factor of 4

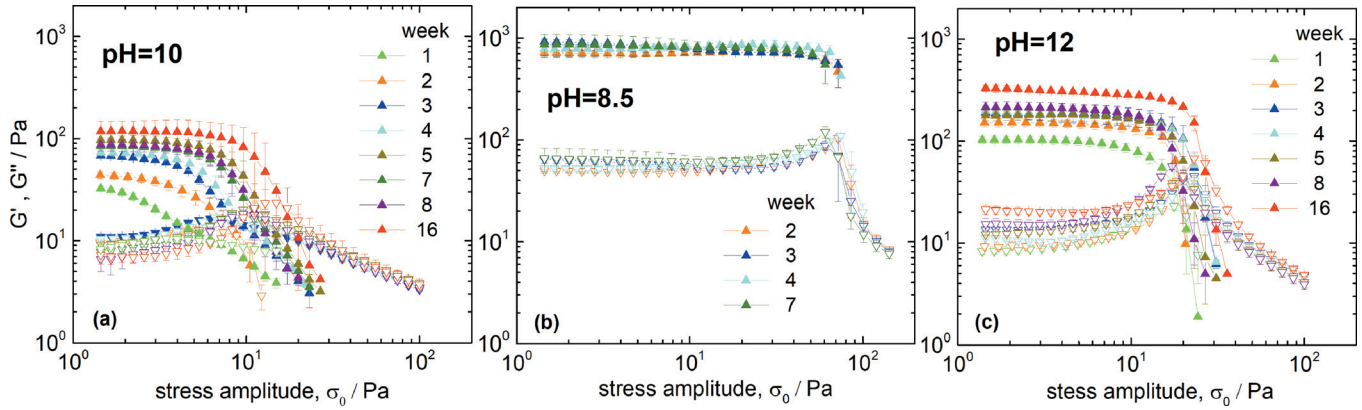

FIG. 4. Amplitude sweep experiments at different aging times for 2 wt. % Laponite dispersions with 10^{-4} M added NaCl (a) at pH = 10, (b) at pH = 8.5 and (c) at pH = 12. Solid up-triangle = G', open down-triangle = G''.

within 16 weeks of storage. Moreover, the mode of failure changes from gradual breakdown for shortly stored samples to catastrophic failure at extended aging times.

Figure 5 compares the time evolution of the normalized storage modulus $G'_{norm} = G'(t_{storage}) / G'(t_{storage} = 0)$ for different repulsive and attractive arrested states. In all cases, the time dependence of G' may be approximated by a power law $G' \sim t^{\alpha}$ with $\alpha = 0.11 \pm 0.03$ for the attractive strong gel states (circle-symbols) in an excellent agreement with the early findings of Willenbacher [36]. In contrast, the weak gels (triangle-symbols) and repulsive glass (square-symbols) exhibit much stronger aging than strong gels. Here, we found $\alpha = 0.74 \pm 0.01$ for the glass with 2 wt. % Laponite and 10^{-4} M NaCl at pH = 10 as well as $\alpha = 0.36 \pm 0.01$ for the weak gels. Aging is assumed to be determined by the mobility of individual layers, and apparently layer mobility is much higher for the layers arrested due to electrostatic repulsion of neighboring layers than for those trapped in contact with attractive neighbors in gel structures.

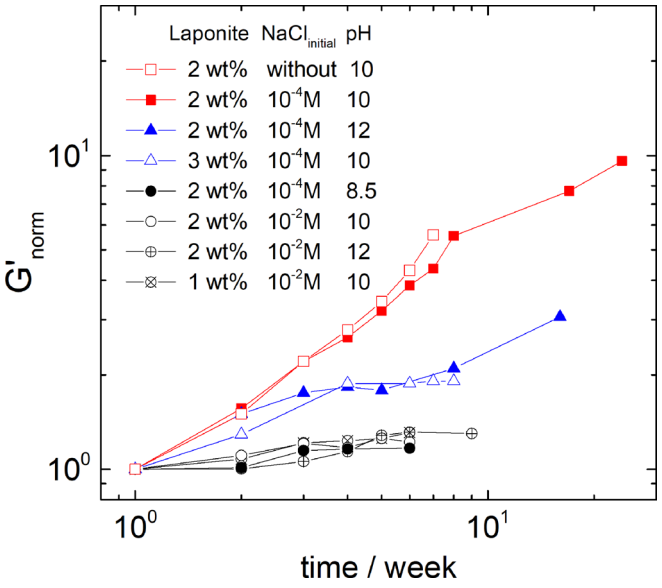

FIG. 5. Normalized plateau moduli as a function of aging time for Laponite dispersions at various solids content and NaCl concentrations at inherent pH of 10, at set pH 12 and 8.5. Circle, triangle, and square symbols represent strong gel, weak gel, and repulsive glass samples, respectively.

D. Broad bandwidth linear viscoelastic relaxation of Laponite dispersions in different arrested states

Jabbari-Farouji *et al.* [33] described the frequency dependence of the shear modulus as a superposition of two power law contributions and found an exponent $\beta \approx 0.7$ characterizing the high frequency relaxation of investigated samples at its inherent pH and in the frequency range from 6 to 6×10^5 rad/s. Here, we combined bulk oscillatory shear and squeeze flow with DWS microrheology to cover the frequency range from 5×10^{-3} to 3×10^6 rad/s. Storage and loss modulus data for 2 wt. % Laponite dispersions with different pH and salt concentration are shown in Fig. 6. This extends the work of Jabbari-Farouji *et al.* [33]. Data obtained with different techniques agree very well, and as expected, G' is essentially constant over more than five decades in frequency but starts to increase at approximately $\omega \approx 10^3$–10^4 rad/s [Fig. 6(a)]. The absolute values of the frequency-independent G' data in the low frequency range demonstrate that at a given Laponite content. The EF-type attractive gel assumed to be formed at pH = 8.5 is stronger than the FF-type arrested state supposed to exist at pH = 12, which in turn has a higher shear strength than the repulsive glass (pH 10). At pH 10 and 12, adding NaCl results in an increase of G', whereas added electrolyte has no effect at pH = 8.5.

At frequencies of approximately 10^3 to 10^4 rad/s G'' also starts to increase strongly according to a power law $G'' \sim \omega^{\beta}$ with $\beta = 0.75 \pm 0.03$ [Fig. 6(b)]. This exponent and the absolute values of G'' are independent of pH or salt concentration within experimental uncertainty. Such a scaling law has been predicted for semiflexible chains such as polymers, wormlike micelles or protein filaments [59,60]. It is attributed to intrinsic relaxation modes of the building blocks of the semiflexible objects and is directly related to the bending stiffness or persistence length of these chains. Accordingly, high-frequency rheology has been used to study the bending stiffness or persistence length of wormlike micelles [49] and protein [61] solutions, which is related to the bending stiffness of the respective chain building blocks, systematically. Here, this characteristic power law may be related to the bending modulus of the single clay mineral layers, which is independent of the mode of arrest in which the layers are trapped.

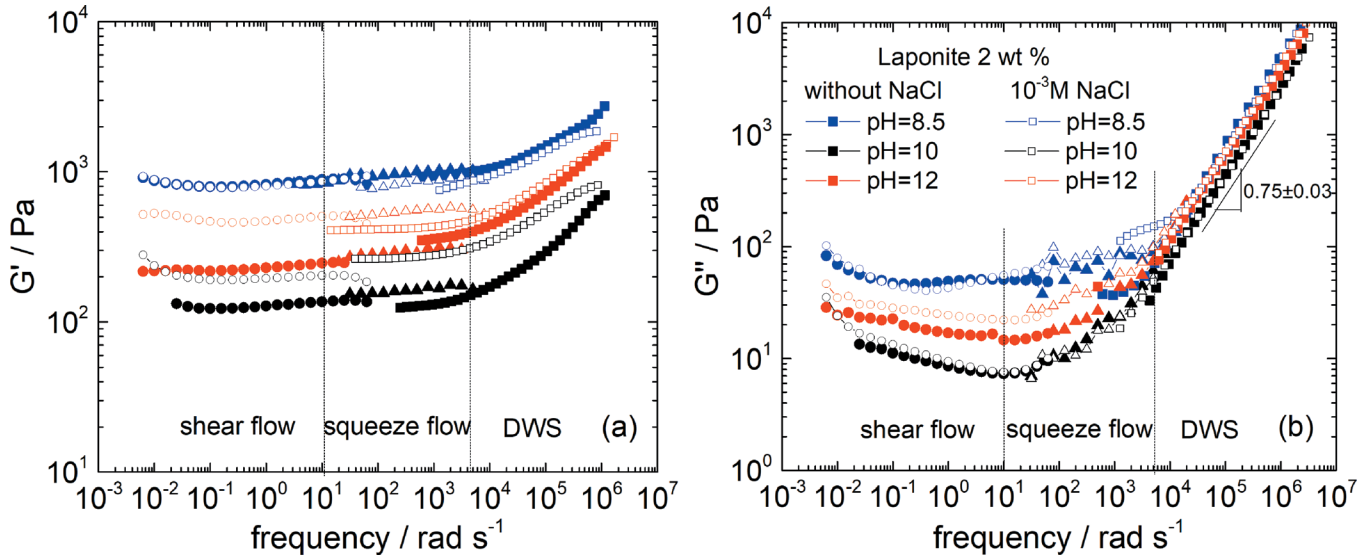

FIG. 6. Linear viscoelastic (a) storage modulus and (b) loss modulus for 2 wt. % Laponite dispersions with and without NaCl at three *p*H values. The broad frequency range was covered with the help of small amplitude oscillatory shear flow (square), squeeze flow (triangle), and DWS experiments (square). All experiments were performed on 10-week-old samples.

E. Microrheology and microstructural heterogeneity

Brownian motion of spherically shaped fluorescent tracer particles embedded in the clay mineral dispersions has been monitored to characterize the change in viscoelasticity and local particle dynamics during the formation of different arrested states. At least 150 tracer particles were tracked simultaneously in a single experiment. From the particle positions in subsequent video images, the mean square displacement MSD(τ) of each particle is obtained as a function of lag time τ, and finally the average MSD(τ) obtained in a single experiment is calculated.

In Fig. 7(a), such average MSD data obtained at different time intervals after sample preparation are shown for a 3 wt. % Laponite dispersion with 10^{-4} M NaCl. Immediately after sample preparation, the MSD of the tracer particles depends linearly on τ, i.e., the tracers diffuse in a viscous environment, the sol state. The slope of the MSD(τ) curves then gradually decreases with increasing waiting time until finally MSD data turn time-independent when the arrested gel state is reached.

The Laplace transform of the average MSD $\langle \Delta\tilde{r}^2(i\omega)\rangle$ is related to the complex shear modulus G^* of the surrounding medium via the generalized Stokes-Einstein equation

$$G^*(\omega) = G'(\omega) + iG''(\omega) = \frac{2k_bT}{\pi di\omega\langle\tilde{\mathbf{r}}^2(i\,\omega)\rangle}, \qquad (2)$$

where T is the temperature, k_b is the Boltzmann constant, and d is the diameter of the tracer particles. This relationship has been used to calculate G' and G'' data from the MSD [50]. The transition from the liquid to the arrested state is clearly visible also from this representation of experimental data [Fig. 7(b)]. Similar results have been reported earlier [32,40], demonstrating that MPT is a versatile, nondestructive way to characterize long-term changes in viscoelastic sample properties even if volatile components are included since the specimens are kept in tightly sealed cuvettes.

Similar experiments have been performed for Laponite dispersions in different arrested states, and structure formation kinetics have been characterized using tracer particles of different size between 0.19 and 1.01 μm. Formation of the repulsive glass and the attractive gel structure for 3 wt. % Laponite dispersed in deionized water and a 10^{-4} M NaCl solution, respectively, is shown in Figs. 8(a) and 8(b). Structure build-up is characterized via the corresponding change in G' and G'' taken at fixed frequency $\omega = 0.6$ rad/s over the waiting time. For comparison, the results from mechanical rheometry are also included.

For the glass sample, the characteristic structure formation time t_c at which $G' = G''$ is independent of the size of the tracer particles, and MPT data are in excellent agreement with bulk rheometry data. This is different from earlier observations [62,63] showing a probe size dependence of tracer diffusivity, but it should be noted that the particle size in these dynamic light scattering and fluorescence recovery after photo bleaching studies is well below the size range investigated here. It should also be noted that the aging of the glasses and gel systems, i.e., the increase in G' for times $t > t_c$ cannot be monitored using MPT. Due to the constraints defined by the noise-to-signal ratio of our setup, the upper limit for the accessible modulus is $G'_{max} \approx 30$ Pa, essentially independent of particle size [50].

A completely different scenario is observed for the sample with 3 wt. % Laponite and 10^{-4} M NaCl considered as a weak gel. In this case, the crossover times t_c from MPT are significantly longer than $t_{c,bulk} = 15$ min obtained from bulk rheometry, i.e., t_c increases systematically with decreasing tracer particle size, and for $d = 0.21$ μm $t_c = 55$ min was found. Similar results were obtained for the sample with 2 wt. % Laponite and 10^{-4} M NaCl; in this case, $t_{c,bulk} = 120$ min and $t_c = 1224$ min were determined using tracer particles with $d = 0.19$ μm. Furthermore, Rich *et al.*

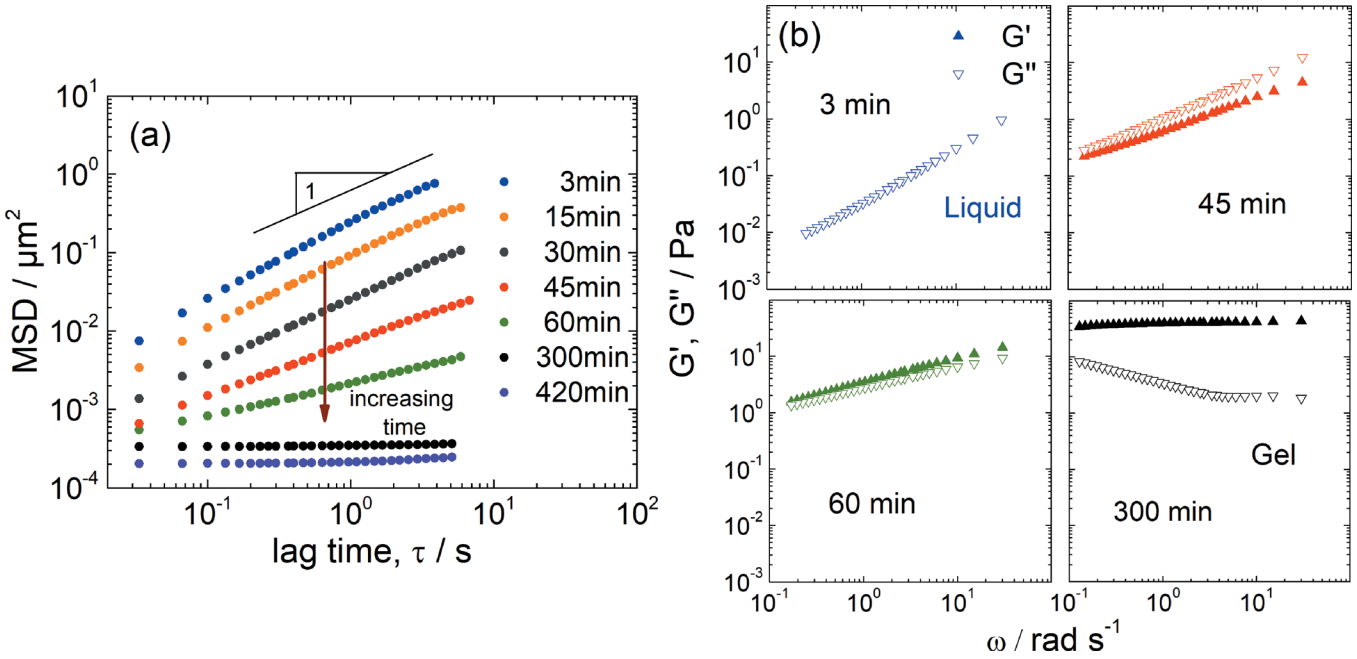

FIG. 7. (a) Mean value of MSD of 0.21 μm tracer particles embedded in a 3 wt. % Laponite dispersion with 10^{-4} M NaCl at pH = 10 at different waiting times. (b) Frequency dependence of the storage and loss moduli of 3 wt. % Laponite dispersion with 10^{-4} M NaCl on the corresponding length scale (0.21 μm) at different waiting times.

[40] found a shift of t_c from $t_{c,bulk} = 6$ min to $t_c = 180$ min at a Laponite concentration of 1 wt. % using 0.11 μm particles, i.e., the delay of the sol-gel transition increases with decreasing clay mineral concentration.

Similar results have been reported previously for Laponite dispersions with solids content between 0.75 and 1.25 wt. % at NaCl concentrations of 1.8×10^{-3} M and 1×10^{-3} M, respectively [32,40], which may also be considered as weak gels. This increase in gelation time with decreasing length scale seems to be consistent with the fractal network model proposed by Pignon *et al.* [64], if layer rearrangements and reorganization of micron-sized clusters assumed to build up the fractal network are considered to occur over long times. On the macroscopic scale, it shows up as slow aging, i.e., weak increase in G' over time as discussed above.

Finally, we have compared macro- and microstructure formation for Laponite gels at pH = 8.5 where EF layer contacts prevail and at pH = 12 where FF is the preferred layer contact mode. As seen in Fig. 8(c), in both cases, gelation is

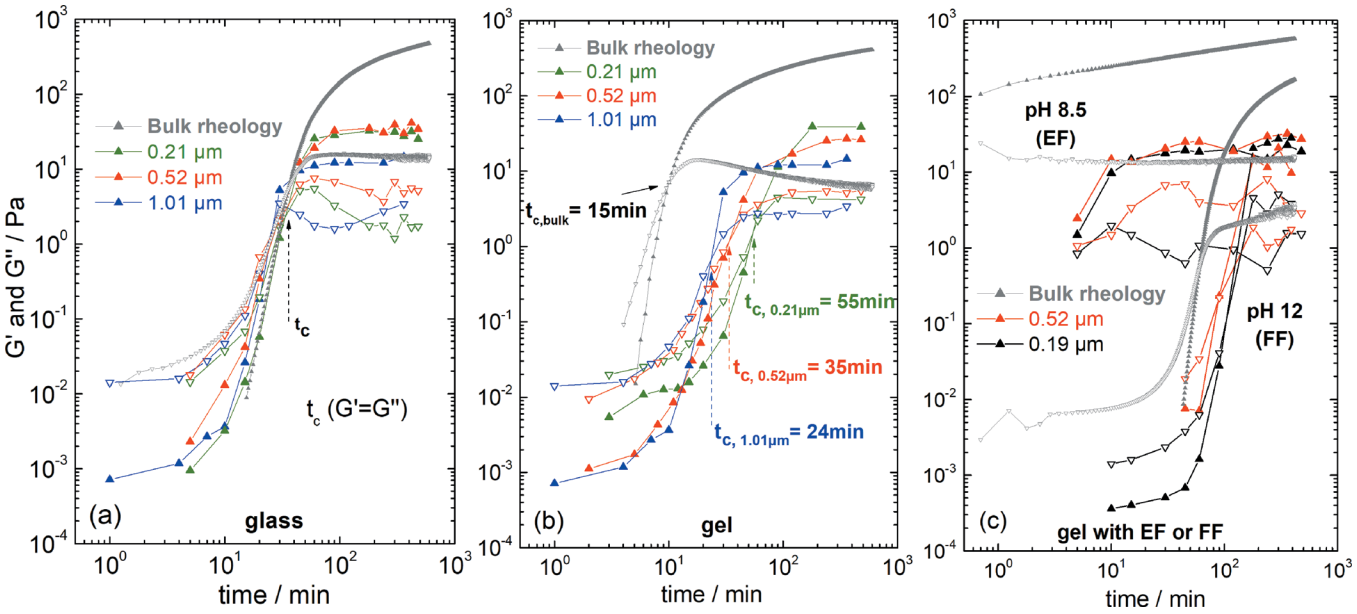

FIG. 8. (a) Glass structure; viscoelastic moduli as a function of time for 3 wt. % Laponite in deionized water at pH = 10. (b) Gel structure; viscoelastic moduli as a function of time for 3 wt. % Laponite in 10^{-4} M NaCl at pH = 10. (c) Gel structure with prevailing EF or FF; viscoelastic moduli as a function of time for 2 wt. % Laponite in 10^{-4} M NaCl aqueous solution at pH = 8.5 (EF) and 12 (FF). G' (solid up-triangle) and G'' (open down-triangle).

significantly delayed at the microscale compared to the macroscale, and structural refinement even occurs in the strong gel obtained at $p\mathrm{H} = 8.5$.

The delayed gelation time observed on the microscale and the corresponding structural refinement seem to indicate a heterogeneity of the attractive gel arrested states, which is not observed in glass systems. MPT is a valuable tool to characterize sample heterogeneities at a submicrometer length scale offering good statistical significance. Oppong *et al.* [32] quantified sample heterogeneity using the non-Gaussian parameter characterizing the deviation of the MSD distribution at a fixed lag time for the ensemble of tracked particles from the Gaussian distribution function to be found in a homogeneous, ergodic system. For the weak gel, they found that this parameter increased sharply until the (microscopic) gelation time was reached and seemed to remain high even at somewhat longer aging times. Similar results were reported by Rich *et al.* [40] using the so-called heterogeneity ratio *HR* as a quantitative measure of spatial heterogeneity obtained by MPT experiments. *HR* is calculated as [65]

$$HR = \frac{M_2(\tau)}{M_1(\tau)^2}, \tag{3}$$

where $M_1(\tau)$ is the estimator for the ensemble average of MSD, and $M_2(\tau)$ is the estimator for the ensemble variance of MSD; both quantities are calculated at a given lag time τ from individual particle trajectories weighted by a factor proportional to their length. For the weak gel, a monotonic increase of *HR* with waiting time was observed even somewhat beyond the gelation point obtained at the length scale of the respective tracer particles [40].

Here, we have investigated the heterogeneity of Laponite dispersions with varying clay mineral content and electrolyte concentrations as well as different *p*H (8.5, 10, and 12), thus including glass and different gel arrested states. We used the parameter *HR* [Eq. (3)] to quantify sample heterogeneity based on MPT experiments with different particle size ($d = 0.19$, 0.21, and 0.52 μm). Figure 9 displays these *HR* data as a function of waiting time t, and the latter is normalized to the microscopic gelation time t_c determined for each sample using the respective tracer particles.

Note that nonzero *HR* values are found even for ideal homogeneous fluids due to limitations of experimental setup and data acquisition [65]. This *HR* threshold has been determined experimentally using a homogenous, highly elastic polymer gel (Puronic F127, $G' = 10^4$ Pa at $T = 20\,^{\circ}\mathrm{C}$), with corresponding horizontal lines for the different particle sizes (Fig. 9). Experimental data for $t/t_c \gg 1$ are close to that threshold for the 0.21 and 0.19 μm particles. For the 0.52 μm particles, the experimental data are significantly lower; the source of this systematic error could not be resolved.

In these MPT experiments, all investigated samples exhibit a pronounced heterogeneity at the sol-gel/glass transition, i.e., at approximately $t/t_c \approx 1$. Consistent with earlier results [33], the glass samples exhibit this heterogeneity only at the length scale of tracer particle size of 0.21 μm but not at larger scales. The degree of heterogeneity seems to be most pronounced for the gel with the EF structure generated at $p\mathrm{H} = 8.5$ and weakest for the gels formed at $p\mathrm{H} = 10$. It should be noted that the HR values are plotted versus t/t_c with t_c obtained for the used tracer particles. This means that heterogeneity is characterized close to the bulk or macroscopic transition to the arrested state for the glass (see Fig. 8) and the FF-type gel at $p\mathrm{H} = 12$. In contrast, the MPT results

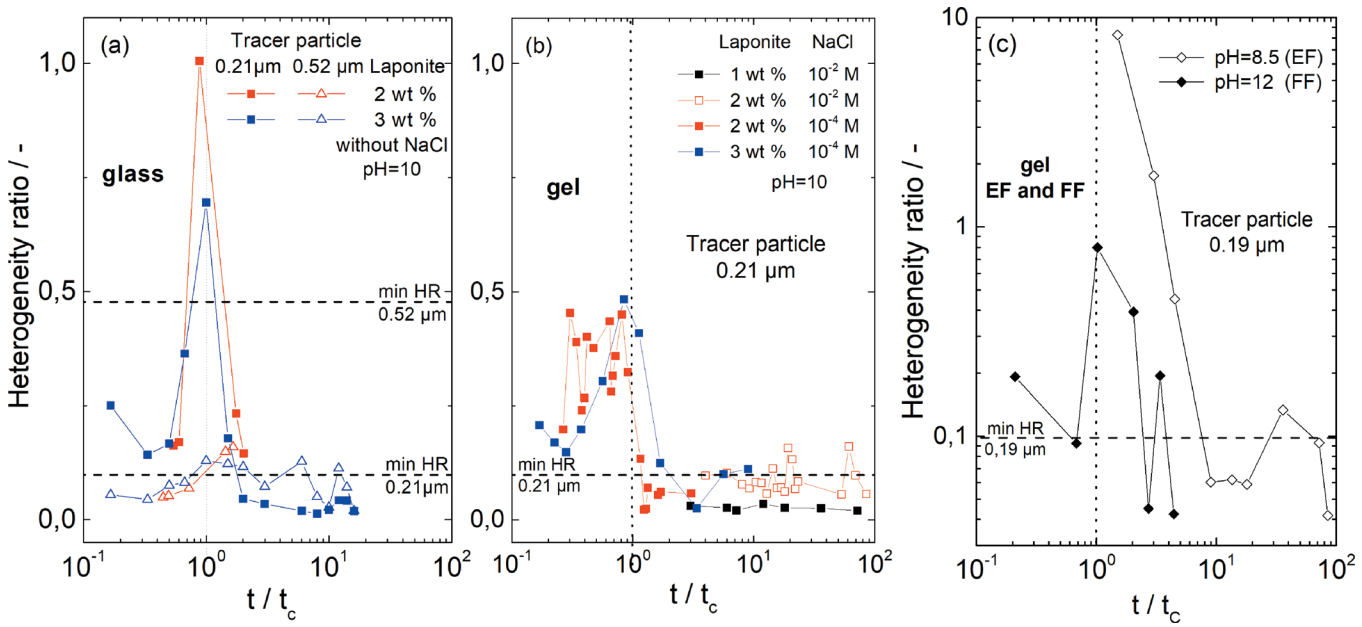

FIG. 9. (a) Heterogeneity ratio (HR) during sol-glass phase transition of Laponite dispersions at $p\mathrm{H} = 10$ measured by the MPT method and using 0.21 and 0.52 μm tracer particles (b) HR during sol-gel phase transition of Laponite dispersions at $p\mathrm{H} = 10$ measured by MPT method and using 0.21 μm tracer particle (c) HR during phase transition of 2 wt. % Laponite in 10^{-4} M NaCl aqueous solution at $p\mathrm{H} = 8.5$ and 12 measured by MPT method and using 0.19 μm tracer particle. The minimal HR for each tracer particle type was determined in homogeneous polymer hydrogel (Pluronic F127) and plotted as a horizontal dashed line. The phase transition point t_c, where G' and G'' are equal, was marked at $t/t_c = 1$ as a vertical dotted line.

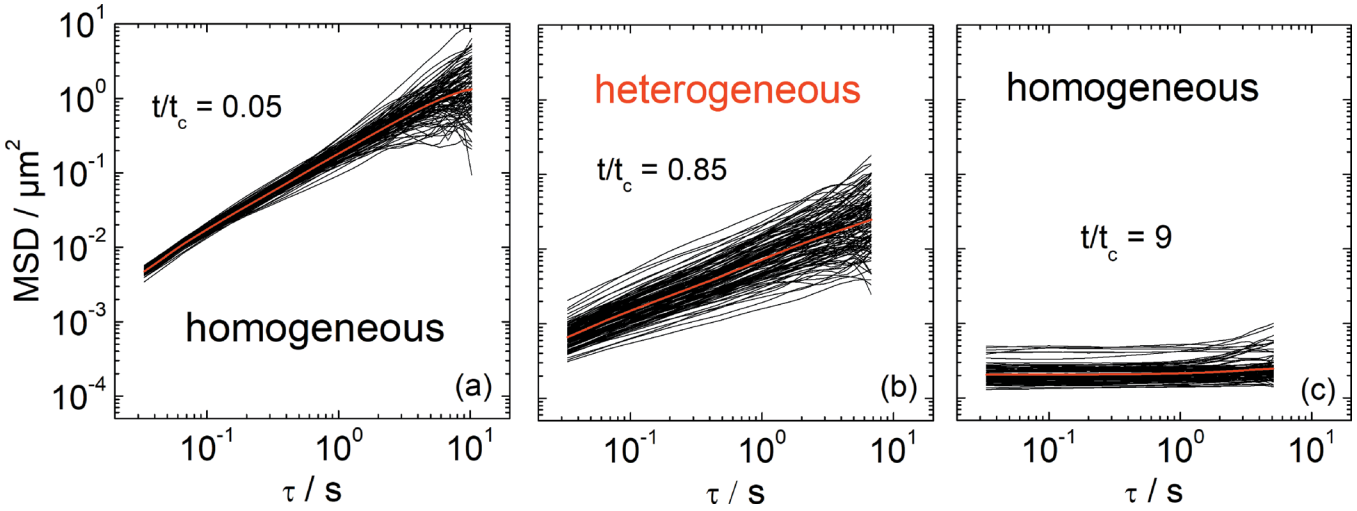

FIG. 10. Ensemble of individual MSD for simultaneously tracked tracer particles (d = 0.21 μm) in a 3 wt. % Laponite dispersion with 10^{-4} M NaCl at different times normalized by crossover time; a broad distribution of MSDs for the heterogeneous structure (b) at $t/t_c \approx 1$ and narrow distributions of MSDs for homogeneous structures (a) at $t/t_c \ll 1$ and (c) at $t/t_c \gg 1$ are clearly visible.

for the weak gels shown in Fig. 9(b) are clearly taken well after the macroscopic gelation occurred, and this might be the reason why the degree of heterogeneity is less pronounced. For the quick gelation system at pH = 8.5 [Figs. 8(c) and 9(c)], the structure may even change during ongoing experiments prohibiting straight forward interpretation.

All arrested states exhibit a uniform structure at a length scale of approximately 10 times the clay mineral layer diameter. Undoubtedly, there is no indication of sample heterogeneity for any of the investigated glasses, weak or strong gels at times $t/t_c \gg 1$. This surprising result is directly visible from the MSD ensembles exemplary shown in Fig. 10.

The tracer particles to be used for reliable MPT experiments are approximately 10 times larger than the Laponite particles. Hence, it is difficult to resolve structural heterogeneities, e.g., addressed in fundamental work about gelation and phase separation in suspension of spherical particle with short-range attraction [66], and this is supposed to be why all arrested states are seen to be homogeneous at $t \gg t_c$.

IV. CONCLUSION

We have investigated the structure formation and aging of Laponite dispersions in different arrested states. By varying clay mineral content (1–3 wt. %), NaCl concentration (up to 10^{-2} M NaCl) and pH (8.5, 10, and 12) glasses, strong and weak gels were formed. Mechanical oscillatory shear rheometry was used to monitor structure formation and aging. Additional insight into structural refinement and sample heterogeneities on a length scale of 0.2–1 μm was obtained from MPT experiments using tracer particles with diameter d between 0.19 and 1.01 μm. The high-frequency linear viscoelastic response of arrested dispersions was determined using oscillatory squeeze flow mechanical rheometry and DWS optical microrheology. The formation of arrested states was characterized by the time t_c at which $G' = G''$ at a fixed frequency. For a given clay mineral content, strong attractive gels (high salt concentration) form much more quickly than weak gels (low salt concentration), particularly the repulsive glass state (no added salt). Gels assumed to have preferred EF layer contacts are stronger and are created much more quickly than gels supposed to have prevailing FF contacts. Aging is much more pronounced for glasses than for attractive gels. For all strong gels, G' increases only weakly for $t \gg t_c$ according to a power law $G' \sim t^{\alpha}$ with $\alpha = 0.11 \pm 0.03$. For the repulsive glasses with 2 wt. % Laponite, $\alpha \approx 0.74 \pm 0.03$ is found, and the exponent for the weak gels ($\alpha \approx 0.36 \pm 0.01$) is in between.

MPT data reveal a structural refinement at the submicrometer length scale during aging, i.e., when the bulk modulus weakly increases, and the characteristic crossover time t_c indicating structure formation increases with decreasing size of the tracers probing their viscoelastic environment. No such refinement is found in glass systems. A pronounced structural heterogeneity occurs during formation of attractive gels and repulsive glasses, i.e., at approximately $t \approx t_c$; this transient heterogeneity is most pronounced for the gel with the HOC structure formed at pH = 8.5. At times $t \gg t_c$ all arrested states appear homogenous at the length scale of 0.2 μm.

Finally, the linear viscoelastic response of all repulsive and attractive arrested states at high frequencies ($\omega > 10^4$ rad/s) exhibits a power law frequency dependence of $G'' \sim \omega^{0.75}$ attributed to internal bending modes of individual layers, which are independent of the type of layer contacts or structures in which these layers are trapped.

ACKNOWLEDGMENTS

The authors gratefully acknowledge the German Academic Exchange Service (DAAD Germany) for financial support. The authors would like to thank Rebekka Maria Cseki for aging measurements and Dr. Laure Delavernhe, Dr. Annett Steudel, and Florian Schnetzer for fruitful discussions.

References

[1] Jabbari-Farouji, S., H. Tanaka, G. H. Wegdam, and D. Bonn, "Multiple nonergodic disordered states in Laponite suspensions: A phase diagram," Phys. Rev. E **78**(6), 061405 (2008).

[2] Levitz, P., E. Lecolier, A. Mourchid, A. Delville, and S. Lyonnard, "Liquid-solid transition of Laponite suspensions at very low ionic strength: Long-range electrostatic stabilisation of anisotropic colloids," Europhys. Lett. **49**(5), 672–677 (2000).

[3] Tanaka, H., J. Meunier, and D. Bonn, "Nonergodic states of charged colloidal suspensions: Repulsive and attractive glasses and gels," Phys. Rev. E **69**, 031404 (2004).

[4] Mourchid, A., E. Lécolier, H. Van Damme, and P. Levitz, "On viscoelastic, birefringent, and swelling properties of laponite clay suspensions: Revisited phase diagram," Langmuir **14**(17), 4718–4723 (1998).

[5] Mongondry, P., J. F. Tassin, and T. Nicolai, "Revised state diagram of Laponite dispersions," J. Colloid Interface Sci. **283**(2), 397–405 (2005).

[6] Ruzicka, B., and E. Zaccarelli, "A fresh look at the Laponite phase diagram," Soft Matter **7**, 1268–1286 (2011).

[7] Ruzicka, B., L. Zulian, and G. Ruocco, "More on the phase diagram of laponite," Langmuir **22**(3), 1106–1111 (2006).

[8] Fossum, J. O., "Physical phenomena in clays," Phys. A Stat. Mech. Appl. **270**(1), 270–277 (1999).

[9] Dijkstra, M., J. P. Hansen, and P. A. Madden, "Gelation of a clay colloid suspension," Phys. Rev. Lett. **75**(11), 2236–2239 (1995).

[10] Nicolai, T., and S. Cocard, "Structure of gels and aggregates of disk-like colloids," Eur. Phys. J. E **5**, 221–227 (2001).

[11] Mori, Y., K. Togashi, and K. Nakamura, "Colloidal properties of synthetic hectorite clay dispersion measured by dynamic light scattering and small angle X-ray scattering," Adv. Powder Technol. **12**(1), 45–59 (2001).

[12] Tawari, S. L., D. L. Koch, and C. Cohen, "Electrical double-layer effects on the Brownian diffusivity and aggregation rate of Laponite clay particles," J. Colloid Interface Sci. **240**, 54–66 (2001).

[13] Bonn, D., H. Tanaka, G. Wegdam, H. Kellay, and J. Meunier, "Aging of a colloidal 'Wigner' glass," Europhys. Lett. **45**(1), 52–57 (1999).

[14] Tombácz, E., and M. Szekeres, "Colloidal behavior of aqueous montmorillonite suspensions: The specific role of pH in the presence of indifferent electrolytes," Appl. Clay Sci. **27**, 75–94 (2004).

[15] Lagaly, G., and S. Ziesmer, "Colloid chemistry of clay minerals: The coagulation of montmorillonite dispersions," Adv. Colloid Interface Sci. **100–102**, 105–128 (2003).

[16] Odriozola, G., M. Romero-Bastida, and F. D. J. Guevara-Rodríguez, "Brownian dynamics simulations of Laponite colloid suspensions," Phys. Rev. E **70**(2), 1–15 (2004).

[17] Jönsson, B., C. Labbez, and B. Cabane, "Interaction of nanometric clay platelets," Langmuir **24**(20), 11406–11413 (2008).

[18] Van Olphen, H., *An Introduction to Clay Colloid Chemistry, for Clay Technologists, Geologists, and Soil Scientists*, 2nd ed. (John Wiley & Sons, New York, 1977).

[19] Dijkstra, M., J.-P. Hansen, and P. A. Madden, "Statistical model for the structure and gelation of smectite clay suspensions," Phys. Rev. E **55**(3), 3044–3053 (1997).

[20] Okamoto, M., P. H. Nam, P. Maiti, T. Kotaka, N. Hasegawa, and A. Usuki, "A house of cards structure in polypropylene/clay nanocomposites under elongational flow," Nano Lett. **1**(6), 295–298 (2001).

[21] Hofmann, U., and A. Hausdorf, "Uber das Sedimentvolumen und die Quellung von Bentonit," Kolloid Zeitschrift **110**(1), 1–17 (1945).

[22] Ramos-Tejada, M. M., F. J. Arroyo, R. Perea, and J. D. G. Durán, "Scaling behavior of the rheological properties of montmorillonite suspensions: Correlation between interparticle interaction and degree of flocculation," J. Colloid Interface Sci. **235**(2), 251–259 (2001).

[23] Durán, J. D. G., M. M. Ramos-Tejada, F. J. Arroyo, and F. González-Caballero, "Rheological and electrokinetic properties of sodium montmorillonite suspensions. I. Rheological properties and interparticle energy of interaction," J. Colloid Interface Sci. **229**, 107–117 (2000).

[24] Zbik, M. S., D. J. Williams, Y. F. Song, and C.-C. Wang, "The formation of a structural framework in gelled Wyoming bentonite: Direct observation in aqueous solutions," J. Colloid Interface Sci. **435**, 119–127 (2014).

[25] Abend, S., and G. Lagaly, "Sol-gel transitions of sodium montmorillonite dispersions," Appl. Clay Sci. **16**, 201–227 (2000).

[26] Giannakopoulos, E., P. Stathi, K. Dimos, D. Gournis, Y. Sanakis, and Y. Deligiannakis, "Adsorption and radical stabilization of humic-acid analogues and Pb2+ on restricted phyllomorphous clay," Langmuir **22**(16), 6863–6873 (2006).

[27] Ruzicka, B., L. Zulian, and G. Ruocco, "Routes to gelation in a clay suspension," Phys. Rev. Lett. **93**(25), 258301 (2004).

[28] Ruzicka, B., L. Zulian, R. Angelini, M. Sztucki, A. Moussaïd, and G. Ruocco, "Arrested state of clay-water suspensions: Gel or glass?," Phys. Rev. E **77**(2), 020402 (2008).

[29] Jabbari-Farouji, S., R. Zargar, G. H. Wegdam, and D. Bonn, "Dynamical heterogeneity in aging colloidal glasses of Laponite," Soft Matter **8**, 5507–5512 (2012).

[30] Jabbari-Farouji, S., G. H. Wegdam, and D. Bonn, "Gels and glasses in a single system: Evidence for an intricate free-energy landscape of glassy materials," Phys. Rev. Lett. **99**(6), 065701 (2007).

[31] Knaebel, A., M. Bellour, J.-P. Munch, V. Viasnoff, F. Lequeux, and J. L. Harden, "Aging behavior of Laponite clay particle suspensions," Europhys. Lett. **52**(1), 73–79 (2000).

[32] Oppong, F. K., P. Coussot, and J. R. De Bruyn, "Gelation on the microscopic scale," Phys. Rev. E **78**(2), 021405 (2008).

[33] Jabbari-Farouji, S., M. Atakhorami, D. Mizuno, E. Eiser, G. H. Wegdam, F. C. MacKintosh, D. Bonn, and C. F. Schmidt, "High-bandwidth viscoelastic properties of aging colloidal glasses and gels," Phys. Rev. E **78**(6), 061402 (2008).

[34] Bonn, D., S. Tanase, B. Abou, H. Tanaka, and J. Meunier, "Laponite: Aging and shear rejuvenation of a colloidal glass," Phys. Rev. Lett. **89**(1), 015701 (2002).

[35] Shahin, A., and Y. M. Joshi, "Irreversible aging dynamics and generic phase behavior of aqueous suspensions of Laponite," Langmuir **26**(6), 4219–4225 (2010).

[36] Willenbacher, N., "Unusual thixotropic properties of aqueous dispersions of Laponite RD," J. Colloid Interface Sci. **182**(2), 501–510 (1996).

[37] Labanda, J., and J. Llorens, "Effect of aging time on the rheology of Laponite dispersions," Colloids Surf. A Physicochem. Eng. Asp. **329**, 1–6 (2008).

[38] Mourchid, A., A. Delville, J. Lambard, E. Lécolier, and P. Levitz, "Phase diagram of colloidal dispersions of anisotropic charged particles: Equilibrium properties, structure, and rheology of Laponite suspensions," Langmuir **11**(6), 1942–1950 (1995).

[39] Kroon, M., W. L. Vos, and G. H. Wegdam, "Structure and formation of a gel of colloidal disks," Phys. Rev. E **57**(2), 1962–1970 (1998).

[40] Rich, J. P., G. H. McKinley, and P. S. Doyle, "Size dependence of microprobe dynamics during gelation of a discotic colloidal clay," J. Rheol. **55**(2), 273–299 (2011).

[41] Bonn, D., H. Kellay, H. Tanaka, G. Wegdam, and J. Meunier, "Laponite: What is the difference between a gel and a glass?," Langmuir **15**(22), 7534–7536 (1999).

[42] Meier, L. P., and G. Kahr, "Determination of the cation exchange capacity (CEC) of clay minerals using the complexes of copper(II) ion

with triethylenetetramine and tetraethylenepentamine," Clays Clay Miner. **47**(3), 386–388 (1999).

[43] Delavernhe, L., A. Steudel, G. K. Darbha, T. Schäfer, R. Schuhmann, C. Wöll, H. Geckeis, and K. Emmerich, "Influence of mineralogical and morphological properties on the cation exchange behavior of dioctahedral smectites," Colloids Surf. A Physicochem. Eng. Asp. **481**, 591–599 (2015).

[44] Awasthi, V., and Y. M. Joshi, "Effect of temperature on aging and time-temperature superposition in nonergodic Laponite suspensions," Soft Matter **5**, 4991–4996 (2009).

[45] Delavernhe, L., M. Pilavtepe, and K. Emmerich, "Cation exchange capacity of natural and synthetic hectorite," Appl. Clay Sci. **151**, 175–180 (2018).

[46] Au, P. I., S. Hassan, J. Liu, and Y. K. Leong, "Behaviour of Laponite gels: Rheology, ageing, pH effect and phase state in the presence of dispersant," Chem. Eng. Res. Des. **101**, 65–73 (2015).

[47] Crassous, J. J., R. Reǵisser, M. Ballauff, and N. Willenbacher, "Characterization of the viscoelastic behavior of complex fluids using the piezoelastic axial vibrator," J. Rheol. **49**(4), 851–863 (2005).

[48] Mason, T. G., and D. A. Weitz, "Optical measurements of frequency-dependent linear viscoelastic moduli of complex fluids," Phys. Rev. Lett. **74**(7), 1250–1253 (1995).

[49] Oelschlaeger, C., M. Schopferer, F. Scheffold, and N. Willenbacher, "Linear-to-branched micelles transition: A rheometry and diffusing wave spectroscopy (DWS) study," Langmuir **25**(2), 716–723 (2009).

[50] Kowalczyk, A., C. Oelschlaeger, and N. Willenbacher, "Tracking errors in 2D multiple particle tracking microrheology," Meas. Sci. Technol. **26**, 015302 (2015).

[51] Crocker, J. C., and D. G. Grier, "Methods of digital video microscopy for colloidal studies," J. Colloid Interface Sci. **179**, 298–310 (1996).

[52] Savin, T., and P. S. Doyle, "Static and dynamic errors in particle tracking microrheology," Biophys. J. **88**(1), 623–638 (2005).

[53] Winter, H. H., and F. Chambon, "Analysis of linear viscoelasticity of a crosslinking polymer at the gel point," J. Rheol. **30**(2), 367–382 (1986).

[54] Tournassat, C., E. Ferrage, C. Poinsignon, and L. Charlet, "The titration of clay minerals: II. Structure-based model and implications for clay reactivity," J. Colloid Interface Sci. **273**, 234–246 (2004).

[55] Struik, L. C. E., *Physical Aging in Amorphous Polymers and Other Materials* (Elsevier Scientific Pub. Co., New York, 1978).

[56] Lifshitz, I. M., and V. V. Slyozov, "The kinetics of precipitation from supersaturated solid solutions," J. Phys. Chem. Solids **19**(1), 35–50 (1961).

[57] Ianni, F., R. Di Leonardo, S. Gentilini, and G. Ruocco, "Aging after shear rejuvenation in a soft glassy colloidal suspension: Evidence for two different regimes," Phys. Rev. E **75**(1), 011408 (2007).

[58] Ruzicka, B., E. Zaccarelli, L. Zulian, R. Angelini, M. Sztucki, A. Moussaid, T. Narayanan, and F. Sciortino, "Observation of empty liquids and equilibrium gels in a colloidal clay," Nat. Mater. **10**, 56–60 (2011).

[59] Morse, D. C., "Viscoelasticity of tightly entangled solutions of semiflexible polymers," Phys. Rev. E **58**(2), R1237–R1240 (1998).

[60] Gittes, F., and F. MacKintosh, "Dynamic shear modulus of a semiflexible polymer network," Phys. Rev. E **58**(2), R1241–R1244 (1998).

[61] Pawelzyk, P., N. Mücke, H. Herrmann, and N. Willenbacher, "Attractive interactions among intermediate filaments determine network mechanics in vitro," PLoS One **9**(9), 1–9 (2014).

[62] Petit, L., C. Barentin, J. Colombani, C. Ybert, and L. Bocquet, "Size dependence of tracer diffusion in a laponite colloidal gel," Langmuir **25**(20), 12048–12055 (2009).

[63] Strachan, D. R., G. C. Kalur, and S. R. Raghavan, "Size-dependent diffusion in an aging colloidal glass," Phys. Rev. E **73**(4), 041509 (2006).

[64] Pignon, F., A. Magnin, J. M. Piau, B. Cabane, P. Lindner, and O. Diat, "Yield stress thixotropic clay suspension: Investigation of structure by light, neutron, and x-ray scattering," Phys. Rev. E **56**(3), 3281–3289 (1997).

[65] Savin, T., and P. S. Doyle, "Statistical and sampling issues when using multiple particle tracking," Phys. Rev. E **76**(2), 021501 (2007).

[66] Lu, P. J., E. Zaccarelli, F. Ciulla, A. B. Schofield, F. Sciortino, and D. A. Weitz, "Gelation of particles with short-range attraction," Nature **453**, 499–503 (2008).